Synthesis and Characterization of Bioreactive-End-Group-Containing Azoinitiators and Their Use for Preparing End-Functionalized Polyvinylpyrrolidone

F. GANACHAUD,[1] A. THERETZ,[1] M. N. EROUT,[1] M. F. LLAURO,[2] and C. PICHOT[1,*]

[1]Unité Mixte CNRS-bioMérieux, ENSL, 46 allée d'Italie, 69364 Lyon cedex 07, and [2]BP 24, LMOPS/CNRS, Solaize, France

SYNOPSIS

New azonitrile initiators carrying *N*-hydroxysuccinimide (ACPS) or biotin derivative (ACP-LC-B) moieties were synthesized from 4,4'-azobis(4-cyanopentanoic acid) (ACPA) with a yield of around 60%. Special care was taken in the assignment of the ^{13}C-NMR resonances of the ACP-LC-B. The kinetic and thermal parameters associated with these initiators were determined by UV spectroscopy and differential scanning calorimetry. The decomposition rate constants (k_d) versus temperature are similar for both ACPA and ACPS initiators and are in good agreement with literature data. The activation energies (E_a) values are 132, 140, and 98 kJ mol^{-1}; and the frequency factors are (ln A) 34, 35, and 25 for ACPA, ACPS, and ACP-LC-B, respectively. Solution polymerization of *N*-vinylpyrrolidone (NVP) in dimethylformamide initiated with ACPA and ACPS showed similar kinetic behavior with a $k_p/k_t^{1/2}$ value of 0.23 (L mol^{-1} s^{-1})$^{1/2}$. This low value and the low molecular weights of the polymers were explained by variations in the initiator efficiencies, as a function of the monomer concentration, as well as by the high chain transfer activity of the solvent. Functionally terminated P(NVP) was evidenced by gel permeation chromatography and an immunoassay test, suggesting that the average number of bioreactive groups per polymer chain was one. © 1995 John Wiley & Sons, Inc.

INTRODUCTION

Azobisnitrile derivative initiators are commonly used in radical-initiated homo- or copolymerizations, either in solution or in emulsion, for many reasons, such as the ability to control their thermal decomposition and the possibility of preparing well-defined polymers with a low dispersity index. Another advantage of such initiators is that they lead to polymer chains with a broad range of functional end groups, especially for two main applications.

1. The synthesis of telechelic polymers, that is low molecular and bifunctionalized prepolymers,[1-3] in order to prepare di- or triblock copolymers.[4,5] To this aim, one requires basic and reactive chemical functionality such as carboxylic[6] or hydroxyl[6,7] groups or bifunctional initiators.[8,9]
2. The synthesis of macroinitiators or INISURFS (surface-active initiators) for use in emulsion polymerization. These initiators are prepared with hydrophilic polymer chains (such as polyethylene oxide,[10-12] polyacrylamide,[13] polyamide,[14] etc.).

There is a need for well-defined functionalized polymers, especially in the biological domain, for the covalent immobilization of biomolecules. The use of initiators bearing suitable reactive groups is well adapted to prepare a variety of functional polymers.

* To whom correspondence should be addressed.

Journal of Applied Polymer Science, Vol. 58, 1811-1824 (1995)
 CCC 0021-8995/95/101811-14

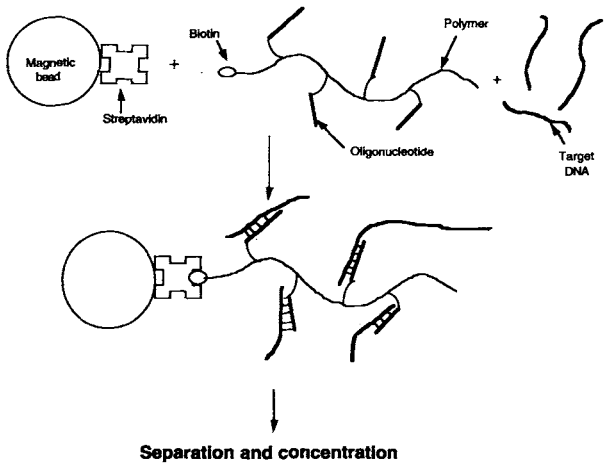

Scheme 1 Hypothetic DNA titration by a novel immunoassay that could be performed by the use of multifunctional copolymer with two different functional groups (biotin at the end and NHS groups along the chain, for example).

4,4′-Azobis(4-cyanopentanoic acid) (ACPA) is one of the most popular azoinitiators used to synthesize adequate functionalized azoderivatives and for which thermal decomposition behavior has been widely described in the literature.[15,16] Many end groups have been fixed on its carboxylic groups, such as substituted amides,[17] acyloxime esters,[18] and even crown ether containing chains, etc.[19] However, to our knowledge, no work has been published on the decomposition rate of ACPA in dimethylformamide (DMF). Furthermore, only one recent publication deals with the quantification of initiator fragments in polyisobutylene polymer chains by NMR spectroscopy.[20] Finally, except for the articles dealing with the incorporation of a biomolecule along the functionalized polymer chain,[21] only one article reporting the chemical incorporation of a phosphatidylcholine head group on azoinitiators has been published recently.[22]

The aim of this study is to conceive a method to capture and isolate DNA fragments, provided by viral cells, in order to concentrate these by the polymerase chain reaction (PCR). This immunoassay could be realized by incorporating biotin end groups in polymer chains, in which complementary oligonucleotides could be bound, in order to link (with a strong affinity) these polymers on a magnetic latex, for example as shown in Scheme 1. Biotin is a model molecule commonly used in biochemistry for its specific binding with avidin and streptavidin.[23]

The purpose of the present study is:

1. to describe the synthesis and characterization of two azobisnitriles prepared from ACPA, containing either an *N*-hydroxysuccinimide ester group (ACPS) or a biotin derivative (ACP-LC-B);
2. to determine the decomposition rate of ACPA, ACPS, and ACP-LC-B in DMF by UV spectroscopy and by differential scanning calorimetry (DSC);
3. to use these initiators in radical-initiated polymerization of *N*-vinyl pyrrolidone (NVP) in DMF for preparing end-functionalized water-soluble polymers; and
4. finally, to perform the titration of the succinimide and biotin polymer end groups by semiquantitative methods (UV and an immunoassay test, respectively).

EXPERIMENTAL

Materials

Deionized water was obtained with a Millipore MilliRo/MilliQ water purification system and used throughout the experiments. Anhydrous DMF from sodium dodecyl sulfate (SDS) was used as received. Dicyclohexyl carbodiimide (DCC, 99% pure from Janssen Chimica) and *N*-hydroxysuccinimide (NHS) provided by Aldrich were used without further purification. Biotin-LC-hydrazide from Pierce and ACPA from Fluka were used after their structure and purity were confirmed by spectroscopic methods. NVP (Aldrich) was distilled under reduced pressure just before use. *ortho*-Phenylene diamine (OPD) was purchased from Sigma and used as received.

Instrumental Methods

Infrared spectra were recorded on a Nicolet 5 PC FTIR spectrometer from Perkin–Elmer. Samples were prepared by means of KBr pellets. ^{1}H- and ^{13}C-NMR spectra were recorded on a Bruker AC 200

Table I FTIR Data of Three Azonitrile Initiators (Wavelength in cm^{-1})

Initiator	NH	OH	C=O	CO—NH
ACPA		3500–2500	1715	
ACPS			1732	
			1786	
			1813	
ACP-LC-B	3292		1701	1540
			1672	1464
			1632	
			1605	

Table II ^{1}H-NMR Data of ACPA and ACPS (Chemical Shifts in ppm)

Initiator	C—CH_3	C—CH_2	OH
ACPA[a]	1.65 (3H, s)	2.3 (4H, m)	≈ 7 (1H, s)
	1.69 (3H, s)[a]		
ACPS	1.69 (3H, s)	3.75 (4H, m)	
	1.75 (3H, s)[a]	2.83 (4H, s)	

Chemical shifts denoted by bold character.
[a] *Cis* and *trans* configuration.

spectrometer at 200 and 50.3 MHz, respectively, for proton and carbon, with tetramethylsilane (TMS) as an internal reference. UV spectrophotometry data were obtained on a Uvikon 930 from Kontron Instrument. Fast atom bombardment mass spectra (FAB) were recorded on a ZAB 2-SEQ mass spectrometer from Fisons Instruments with a Cs ion gun, using *m*-nitrobenzyl alcohol as a matrix.

Azonitrile Derivatives Syntheses

ACPS

Anhydrous DMF (200 mL) was poured into a 500-mL reaction vessel and purged with nitrogen for 1 h. ACPA (3.5 g, 12.5 mmol) and NHS (5.766 g, 37.5 mmol, 1.5 equiv for two acid functions) were introduced into the reactor and the mixture was magnetically stirred at ca. 0°C. DCC (7.764 g, 50 mmol, 2 equiv) was gradually added to the solution over 30 min. The reaction was allowed to proceed for 8 h. The obtained white precipitate (dicyclohexyl urea or DCU) was filtered. Diethyl ether (200 mL) was poured onto the solute, and this solution was kept overnight at 4°C. The resulting precipitate was filtered and dried under reduced pressure; this step was repeated three times. Finally, the residual solution was poured into a separating funnel with saturated NH_4Cl aqueous solution (400 mL) and the white precipitate located at the interface was filtered off and dried. All these last fractions were crystallized in DMF/diethyl ether (1/10 weight ratio) to remove any residual DCU. The yield of the reaction was 60%.

ANAL. Calcd for $C_{20}H_{22}N_6O_8$: C, 50.63%; H, 4.64%; N, 17.72%; O, 27%. Found: C, 50.26%; H, 4.86%; N, 17.78%; O, 26.7%. FTIR: see Table I. ^{1}H- and ^{13}C-NMR: see Tables II and III, respectively.

ACP-LC-B

ACPS (4.75 mg, 10 μmol) and biotin-LC-hydrazide (5.6 mg, 15 μmol, 0.75 equiv for two end groups) were introduced with anhydrous DMF (5 mL) in a 10-mL Falcon tube and stirred overnight at 25°C on a rotating wheel. The solution was poured in diethyl ether (70 mL); the resulting green precipitate was filtered, and dried under reduced pressure. The yield of the reaction was 60%.

ANAL. Calcd for $C_{44}H_{74}N_{14}O_8$: C, 53.5%; H, 7.1%; N, 19.9%. Found: C, 53.5%; H, 7.07%; N, 18.37%. FTIR: see Table I. ^{13}C-NMR: see Table IV. FAB (+): 988.0 $(M + H)^+$.

ACPS Succinimide End Groups Determination

This measurement has already been successfully carried out using UV spectroscopy.[24] ACPS reacts with an excess of aqueous NH_4OH (0.1*N*), and releases hydroxysuccinimide anions (absorbance at λ_{max} = 260 nm) (Scheme 2).

The validity of using Beer's law was verified as follows: NHS (11.5 mg, 100 μmol) was placed in a solution of DMF (10 mL) and NH_4OH 0.1*N* (10 mL, 20 equiv) and introduced in 980 mL of bidistilled water. A series of dilutions of the NHS solution were prepared, introduced in a 1-cm path length cell and the optical density was measured at 260-nm wavelength. ACPS end groups titration was performed in the same way. A solution prepared as de-

Table III ^{13}C-NMR Data of ACPA and ACPS

Initiator	1	2[a]	3	4[a]	5[a]	6	7 + 8	9 + 10[a]
ACPA[b]	71.6	22.8	118.0	28.7	32.4	172.5		
		23.0[c]						
ACPS[d]	72.5	23.3 (*trans*)	118.5	28.8	32.8	168.6	170.7	26.2

Chemical shifts in ppm; carbon numbers refer to those shown in Scheme 3.
[a] Confirmed by a DEPT 135 pulse sequence (distorsionless enhancement by polarization transfer).
[b] Sampled in DMSO-d6.
[c] Two singlet from *cis* and *trans* configuration, respectively.
[d] Sampled in DMF-d7.

Table IV Assignment of ACP-LC-B ^{13}C Resonances by Increment Method (in DMSO-d6, with TMS as Standard)

Initiator	a	b	c	d	e	f	g	h	i	j	k
Biotin[a]	166.0	60.4	62.2	39.9	55.5	27.9	28.5 (26.4)[b]	25.8 (24.7)[b]	37.5 (34.1)[b]	184	
Biotin hydrazine	162.6	59.0	60.9	—[c]	55.3	27.9	28.1	25.1	33.1	171.4	
Biotine-LC-hydrazine	162.6	59.0	60.9	—[c]	55.3	27.9	28.1	24.8	38.1	171.6	35.1
ACP-LC-B	162.2	59.0	60.9	—[c]	55.3	27.9	28.1	—[d]	38.3	171.7	35.1

Initiator	l	m	n	o	p	1	2	3	4	5	6
Biotin											
Biotin hydrazine											
Biotine-LC-hydrazine	28.8	26.0	25.2	33.2	171.4						
ACP-LC-B	28.7	26.0	25.2	33.2	170.9	71.9	23.1	118.0	—[d]	32.9	168.9

[a] From Breitmaier and Voelter,[29] in D_2O.
[b] Estimated values calculated by the increment method.
[c] Masked by the DMSO resonances.
[d] Not assigned.

scribed above but containing 50 μmol of ACPA instead of NHS was introduced in the reference cell. The same quantity of ACPS was diluted in the aqueous NH_4OH solution and introduced in the sample cell and the optical density measurement at 260 nm gave the total amount of NHS released.

Decomposition Rate Measurement of ACPA (UV Spectroscopy) and ACPS and ACP-LC-B (DSC)

The decomposition rate of ACPA was determined by a UV spectrometric method, with anhydrous DMF as the standard. The absorption curve for ACPA was determined and the validity of using Beer's law was established at 350 nm between 0 and 5.10^{-3} mol L^{-1}. The cells were heated via a thermoregulated system keeping the temperature at ±0.5°C. One milliliter of a 5.10^{-3} mol L^{-1} solution of ACPA in DMF was introduced into the sample cell. After an initial period needed to reach a constant temperature, the ACPA thermal decomposition rate in DMF was determined by measuring the decreasing absorption at 350 nm. The first-order decomposition rate constant, k_d, was calculated from

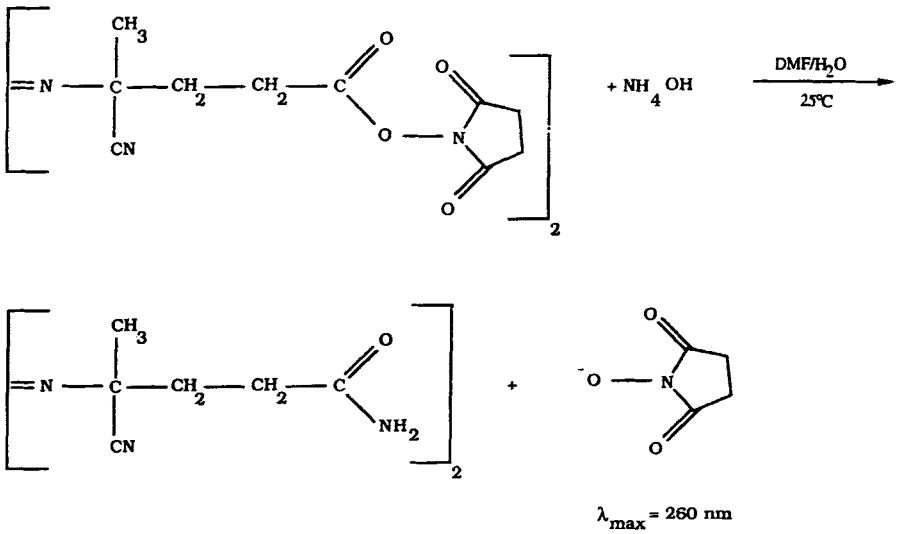

Scheme 2 Principle of the titration of succinimide groups provided by ACPS.

$$k_d = \frac{1}{t} \cdot \ln\left(\frac{D_0}{D_t}\right) \quad (1)$$

where D_0 and D_t represent the absorbance at time 0 and t, respectively.

ACPS and ACP-LC-B decomposition rate measurements could not be performed by UV spectroscopy due to the great absorbance of the molecule cycles at 260 nm. A Mettler-type differential scanning calorimeter was used to determine the kinetic data of the two azoinitiators according to Nuyken's method.[25] A small amount of ACPS and ACP-LC-B were introduced into a pressure tight container made from aluminum, in the absence of solvent. The temperature range 80–200°C was investigated. The heating rate was 10 K min^{-1}. Figure 1 shows a typical DSC trace for the decomposition of ACPS. A computer program allows us to deduce the Arrhenius plot from these curves, giving the activation energy E_a directly, and the frequency factor A.

Homopolymerization of NVP with Azoderivatives

Procedure

Although the amounts of NVP introduced in the reactor were different according to the type of investigated initiator, polymerization runs were performed under the same experimental conditions: 80 mL of DMF were introduced in the reactor and purged with nitrogen for 2 h at 70°C. The solution was magnetically stirred. Then various amounts of monomer were added by means of a syringe pump. Reaction time began with the addition of the initiator dissolved in a small quantity of solvent (10 mL) and then the volume was completed to 100 mL. After 8 h of reaction time, the polymer (PVP) was precipitated in diethyl ether (500 mL) upon vigorous stirring. The precipitate was then quickly filtered, dried in vacuum, and stored under dry atmosphere to avoid water rehydration.

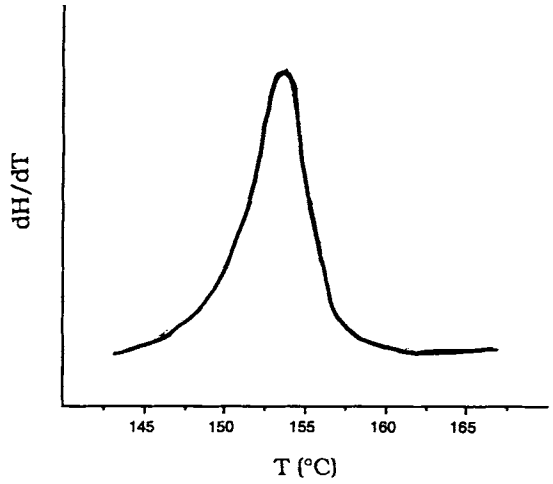

Figure 1 Typical DSC trace for ACPS with a heating rate of 10 K min^{-1}.

Kinetic Studies

Two milliliters were withdrawn from the reaction mixture every 30 min, in which the polymerization reaction was inhibited by adding hydroquinone and by placing the samples in a ice bath. Residual monomer amounts were measured by gas chromatography (GC) to establish monomer consumption rates versus time. GC analysis was performed using DELSI equipment (DI 200) with a Carbowax column (10% carbowax 20M on a chromosorb 80/10 mesh, 1 m length) using a flame ionization detector (oven temperature 180°C, injector and detector temperature 250°C). The amount of residual NVP (in moles) was calculated from the peak areas, using DMF as an internal standard, according to the relationship:

$$A_t = \left(\frac{\text{Area}_t}{\text{Area}_0}\right) \times A_0 \quad (3)$$

where A_0 and A_t represent the total amount of residual NVP at time 0 and t, respectively.

Polymer Characterization

Gel-permeation chromatography (GPC) was carried out to characterize the final polymer molecular weight. A Waters device was used equipped with a Ultrahydrogel 500 column. Samples of PVP (1 gL^{-1}) were prepared in a phosphate buffer of pH 6.8. The eluent was phosphate buffer at a flow rate of 0.5 mL/min, and detection was performed by checking the optical density at 220 and 260 nm simultaneously (using a Waters 484 UV spectrometer detector). The number-average molecular weights ($\overline{M_n}$) were calculated from a calibration using a series of narrowly distributed polysaccharidic standards.

Polymer End Groups Analysis

Polymer end groups were titrated in the ACPS and ACP-LC-B initiated polymerizations.

Succinimide Titration

Succinimide anions were released from the polymer initiated by ACPS as previously described, and were

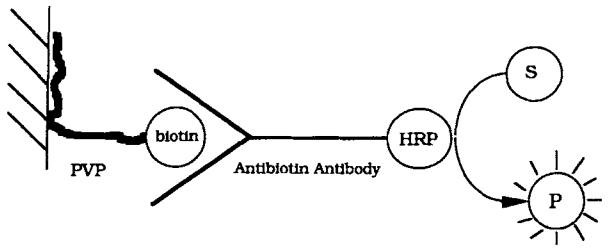

Scheme 3 Principle of the titration of biotin functionalized polymers by an immunoassay method. (S and P are the enzymatic reaction substrate and product respectively; HRP, horse radish peroxidase).

detected by GPC with a UV detection at 220 and 260 nm. NHS amounts, obtained from peak areas, were compared to theoretical values, calculated for one succinimido end group per polymer chain.

Biotin Titration

Biotin end groups were titrated by an immunoassay described in Scheme 3. PVP (100 μL of solutions in a PBS 3X buffer,[1] concentration ranging from 0.01 to 1 ng/μL) initiated by ACP-LC-B or ACPS (reference) was coated on a microplate, and incubated for 2–2.5 h at 37°C. The plate was then washed with PBS Tween (three times). A mouse monoclonal antibiotine antibody-HRP (horse radish peroxidase) conjugate (100 μL of 1/100 and 1/250 dilutions in a PBS 3X/PBS horse serum, 90/10, buffer) was reacted specifically on the biotin end groups during 1–1.25 h at 37°C. After three washing steps with PBS Tween, the HRP antibody was then engaged in a detection enzymatic reaction[26]: the substrate was mixed with 4 mg of OPD with 1 mL of buffer (phosphate 100 mM, citrate 50 mM, pH 4.93) and 1 μL hydrogen peroxide added, as a coreagent, just before the injection of this solution in the microplate (100 μL). The reaction was neutralized after 10 min by addition of an aqueous H_2SO_4 solution (1N, 100 μL). The final product was titrated by direct colorimetric measurement at 492 nm on a microreader AXIA (bioMérieux S.A). [1]PBS 3X: Phosphate buffer, 0.15M; NaCl, 1.37M; pH 7.4.

RESULTS AND DISCUSSION

Synthesis and Characterization of ACPS and ACP-LC-B

The strategy followed for the synthesis of the two initiators is shown in Scheme 4. ACPS purification was successfully achieved after several precipitations, due to the concomitant precipitation of ACPS and the residual dicyclohexyl urea (DCU) in diethyl ether. The weight ratio of DMF/diethyl ether must be carefully controlled (typically 1/10) to reach a good yield. Alternatively, this synthesis could be done in two steps using a chloride intermediate as recently described.[27]

ACPS and ACP-LC-B were characterized by FTIR and NMR spectroscopy. Table I gives the infrared data of ACPA, ACPS, and ACP-LC-B, respectively. The disappearance of the OH band between 3500 and 2500 cm^{-1}, and the appearance of new absorption peaks corresponding to the C=O groups around 1700 cm^{-1}, confirm that the synthesis of each of the two initiators was achieved.

^{1}H- and ^{13}C-NMR spectroscopic measurements were also performed; the chemical shifts for ACPA and ACPS are collected in Tables II and III, respectively. These results confirm that synthesis of ACPS gives *trans* configuration diazo molecules preferentially. The *cis/trans* configuration ratio of the azo species was calculated from ^{1}H-NMR data and was found to be around 49/51 for ACPA and $\approx$ 20/80 for ACPS. The only obvious *trans* configuration should exist in the ACP-LC-B molecule.

From the elemental analyses of ACPS and ACP-LC-B compared with the theoretical values, it may be concluded that the functionalization of ACPA was achieved at both ends of the molecule. Mass spectrometry measurements of ACP-LC-B confirm this result (see Experimental).

A UV spectroscopic method was used for the titration of succinimido end groups (see Experimental). Utility of Beer's law was verified between 0 and 10^{-4} mol L^{-1} (Fig. 2), giving an absorption coefficient ε_{NHS} = 7700 L mol^{-1} cm^{-1}, which is slightly different from that reported in the literature[24] (ε_{NHS} = 9700 L mol^{-1} cm^{-1} in pure water). This can be explained by the amount of DMF added in the sample and the great excess of aqueous NH_4OH introduced (20 equiv instead of 1, to increase the rate of the aminolysis reaction). In any case, the titration of ACPS end groups confirmed the total functionalization of ACPA by NHS (see Fig. 2).

^{13}C-NMR Study of ACP-LC-B Initiator

Due to the great number of very similar hydrogens in the molecule, the ^{1}H-NMR spectrum of ACP-LC-B recorded at 200 MHz cannot be exploited. On the other hand, the ^{13}C spectrum gives sufficient resolution to be studied. We achieved the assignment of all the peaks by comparison with estimated chemical shifts calculated with additivity rules using incre-

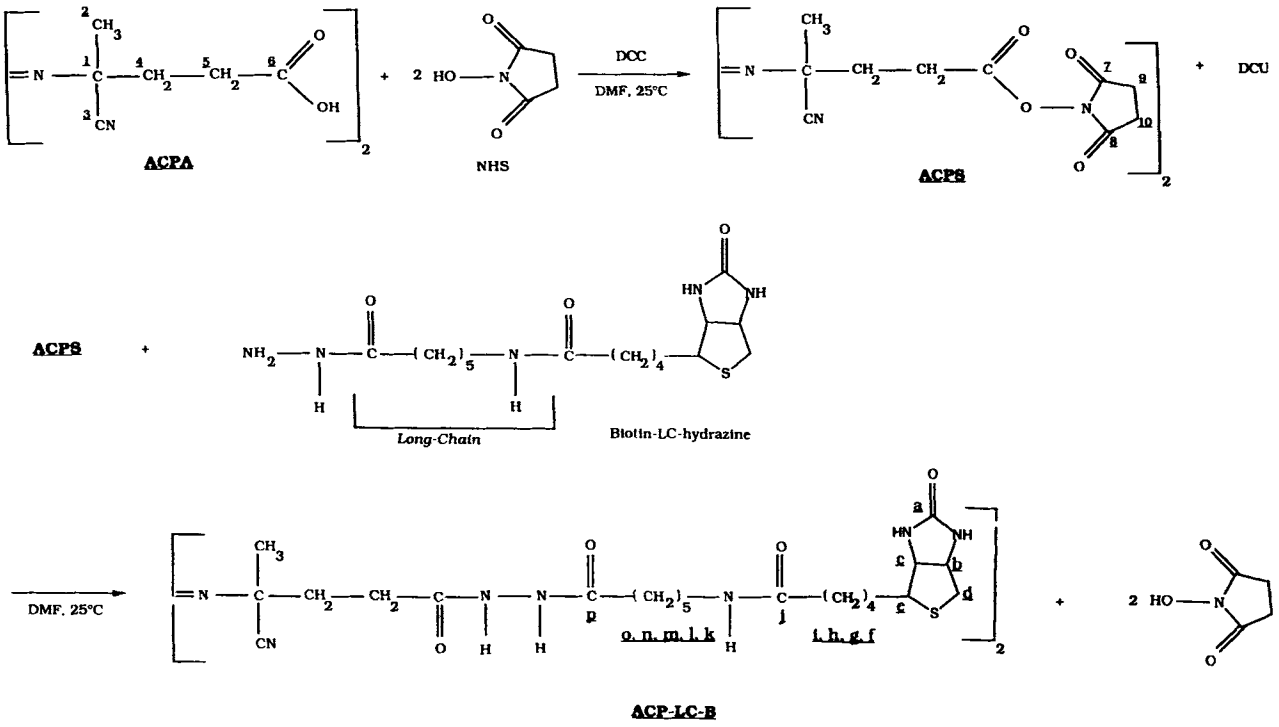

Scheme 4 Syntheses of azonitrile derivatives.

ment values[28] that take into account the surrounding environment of each examined carbon. Three steps were needed.

1. Biotin spectrum: the ^{13}C-NMR spectrum of biotin shows a crowding of signals between 25 and 30 ppm. The literature provides the complete assignment in D_2O thanks to the J-resolved two-dimensional ^{13}C-NMR matrix.[29]
2. Biotin hydrazide spectrum: only the two carbons near the hydrazide group have a different chemical shift; these were assigned in comparison with the estimated values provided by the increment method.
3. Biotin-LC-hydrazide spectrum: it was used in the same way to assign peaks from the ACP-LC-B, given in Table IV.

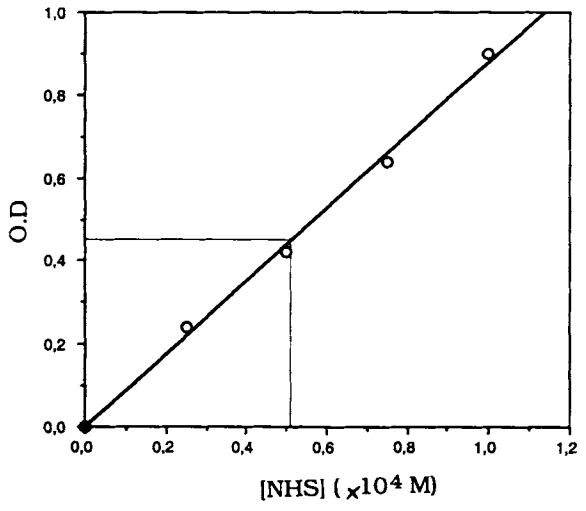

Figure 2 Calibration curve from various NHS solutions for the ACPS NHS end groups by UV spectroscopy. The OD measured corresponds to the titration of $10^{-5}M$ ACPS (i.e., 5 $10^{-4}M$ of free NHS after aminolysis).

Decomposition Rate Measurement of ACPA by UV Spectroscopy

The thermal decomposition of ACPA was investigated in DMF over the temperature range 71.7–93.5°C, by following the disappearance of the azo bond absorbance at 350 nm. The verification of Beer's law was checked at λ = 350 nm at 25°C, for solutions of ACPA in DMF ranging from 0 to 10^{-2} mol L^{-1}. The absorbance coefficient was found to be ε = 14.3 L mol^{-1} cm^{-1}. A plot of the data according to eq. (1) is reported in Figure 3 showing that the rate of decomposition follows first-order law kinetics, as expected.

The rate constants k_d were calculated to be 7.25 10^{-5}, 9.62 10^{-5}, 1.09 10^{-4}, 1.43 10^{-4}, 2.12 10^{-4}, 3.53

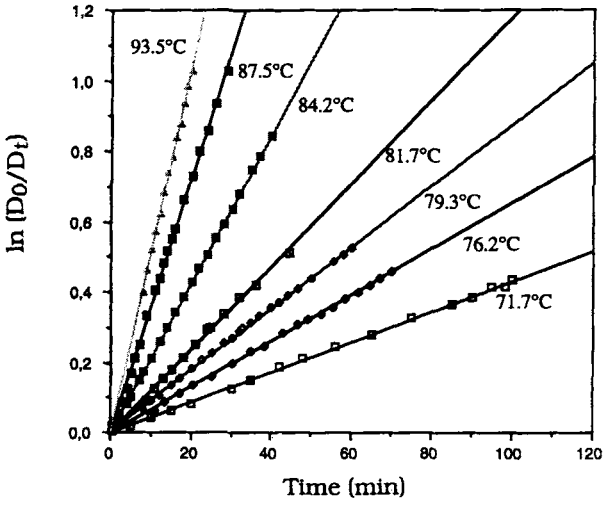

Figure 3 Plots according to eq. (1) when ACPA was decomposed in DMF at various temperatures.

10^{-4}, 5.96 10^{-4}, and 8.65 10^{-4} for 71.7, 75, 76.2, 79.3, 81.7, 84.2, 87.5, and 93.5°C, respectively.

These values allowed us to deduce from the Arrhenius equation [eq. (4)] the frequency factor A and the activation energy E_a needed to decompose this initiator:

$$k_d = A \cdot \exp\left(-\frac{E_a}{RT}\right) \quad (4)$$

where R is the gas constant. The Arrhenius plot of the rate constant (ln k_d versus $1/T$) is reported in Figure 4, from which ln A and E_a were estimated. These former values are given in Table V. Data on

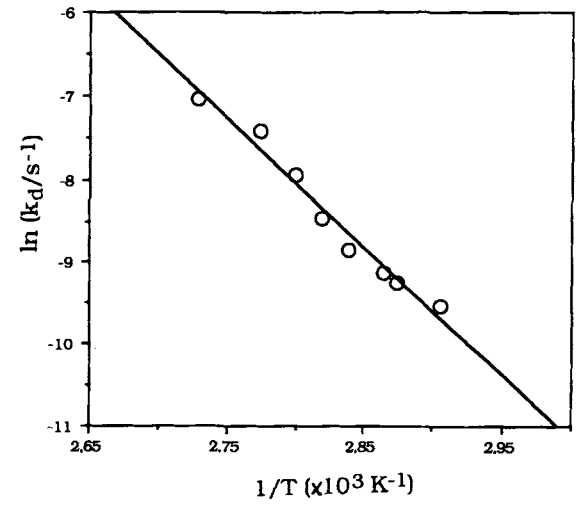

Figure 4 Arrhenius plot for the decomposition of ACPA in DMF.

Table V Activation Energies (E_a) and Frequency Factors (ln A) for Three Initiators

Initiator	E_a (kJ mol^{-1})	ln(A/s^{-1})
ACPA[a]	132 ± 5	36 ± 1
ACPS[b]	140 ± 8	35 ± 2
ACP-LC-B[b]	97 ± 8	25 ± 2
ACPA[c]	132.9 ± 1.1	36.4

[a] UV measurements.
[b] DSC measurements.
[c] Values in D_2O, from Idage et al.[17]

the decomposition rate of ACPA in acetone[30] and H_2O,[17] either in the acidic or the carboxylate form, have already been published; but none showed an influence of pH or solvent on the Arrhenius constants, which is confirmed in our case with DMF.

Decomposition Rate Measurement of ACPS and ACP-LC-B by DSC

UV spectra of ACPS and ACP-LC-B show intense absorptions around 260 nm, as mentioned above. Therefore, the thermal decomposition of these two initiators cannot be followed by the UV method due to the interferences of the NHS group and biotin cycle absorbances at the investigated wavelength (350 nm).

Furthermore, a typical series of ^{1}H-NMR (200 MHz) spectra were recorded during the course of a thermal decomposition of ACPS in DMF-d7 [Fig. 5(a–c)]. Various initiator derived products give rise to different methylenic resonances slightly more shielded than initial (1)-methylenic resonance at δ = 1.870 ppm. The same process occurs for (3)-methylenic protons (the initial triplet is centered at δ = 2.630 ppm). Due to overlapping of initiator resonances from residual and decomposed products, ^{1}H-NMR data are not helpful to determine the ACPS decomposition rate.

Therefore, the decomposition rates of ACPS and ACP-LC-B were followed by DSC. This method is quite convenient because only one experiment allows us to obtain the rate constants at various temperatures, as explained in the Experimental Section; moreover, a small amount of sample is required.[10,18,25,31] The activation energy E_a and the logarithm of the frequency factor ln$A$ are reported in Table V.

It can be concluded from these results that ACPA and ACPS initiators exhibit almost the same decomposition rate constants. This is generally true

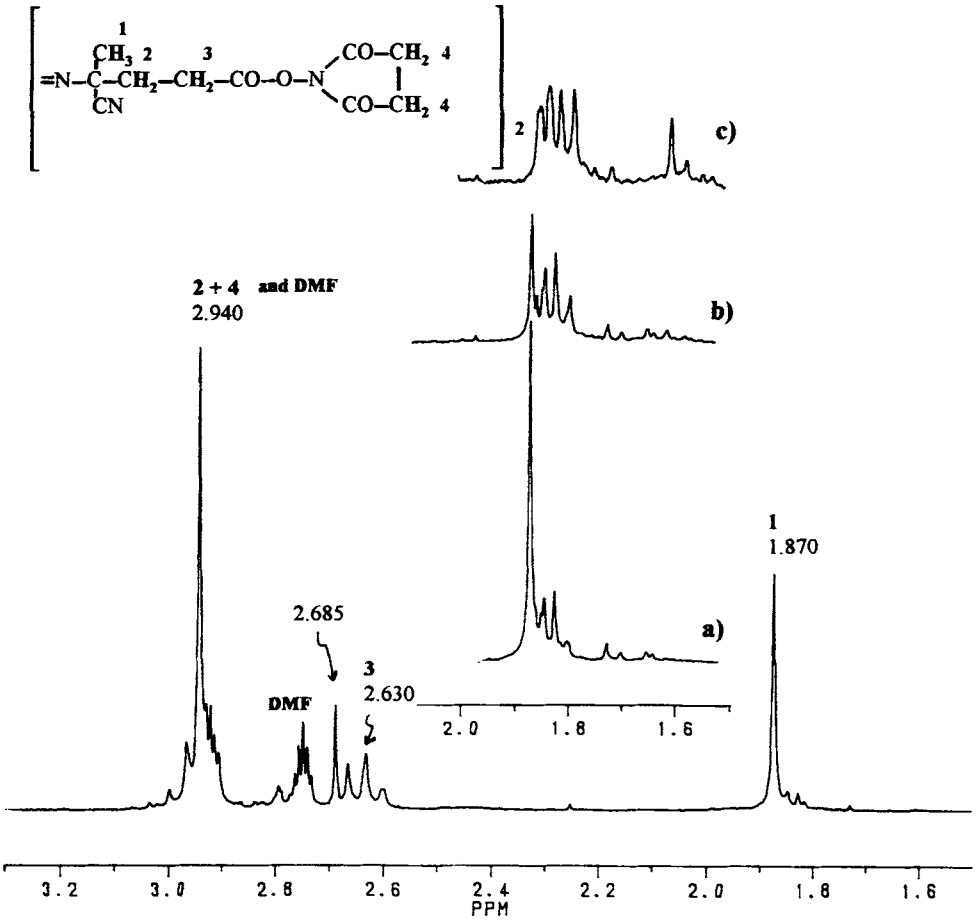

Figure 5 ^{1}H-NMR spectrum of ACPS in DMF-d7; NMR monitoring during thermal decomposition at 75°C: (a) after 50 min; (b) 1 h 43 min; (c) 2.5 h.

for an initiator that does not contain sterically hindered end groups,[25] contrary to the case of the biotine derivative for which the decomposition rate is higher, as also reported in the literature.[18,31,32]

Preparation of Bioactive End Functionalized PVP Chains

Kinetic Studies and Characterization of Polymers

NVP monomer was polymerized in DMF at 70°C using each of the three azonitrile initiators, according to various experimental conditions as indicated in Table VI.

Kinetic results were reported as conversion versus time curves to compare the different polymerization runs (Fig. 6).

First, it appears that NVP polymerization exhibits the same curve shape whether ACPA or ACPS is used, that suggests that ACPS initiated polymerization behaves similarly to that with ACPA. On the contrary, it seems that ACP-LC-B initiated polymerization proceeds at a slower rate that can be explained either by the effect of the sterically hindered biotin group on the azoinitiator efficiency or by transfer reactions of the ACP-LC-B molecule (bearing labile protons) onto the polymer.

Furthermore, $k_p/k_t^{1/2}$ values for NVP in DMF were obtained from the graph reported in Figure 7, according to the well-known equation:

$$\ln \frac{[M_0]}{[M_t]} = 2k_p \cdot \left(\frac{f \cdot [I_0]}{k_d \cdot k_t}\right)^{1/2} \left(1 - \exp\left(\frac{-k_d \cdot t}{2}\right)\right) \quad (5)$$

where: k_p, k_t, and k_d are absolute rate constants for propagation, termination, and initiator decomposition, respectively; f is the initiator efficiency; $[M_0]$ the initial monomer concentration; $[M_t]$ the residual monomer concentration at t; and $[I_0]$ the initial initiator concentration. The decomposition rate constants at 70°C, calculated from the Arrhenius equa-

Table VI Recipes Used in NVP Polymerizations

References	Initiator Type	Amount of Initiator		Monomer (mol L^{-1})
		g L^{-1}	10^3 mol L^{-1}	
GAF1	ACPS	0.475	1.10	0.25
GAF2	ACPS	0.475	1.10	0.62
GAF3	ACPS	0.500	1.12	1.98
GAF4	ACPA	0.500	1.78	2.03
GAF5	ACP-LC-B	0.113	1.14	0.23

tion, eq. (4), are $k_d = 4.9\ 10^{-5}\ s^{-1}$ for ACPA and ACPS and $k_d = 1.2\ 10^{-4}\ s^{-1}$ for ACP-LC-B.

Final conversions, the corresponding number-average molecular weights, and the $k_p/k_t^{1/2}$ parameter for NVP in DMF are reported in Table VII (assuming that ACPA and ACPS initiator efficiency at high monomer concentration is approximately that given for bulk polymerization,[33] i.e., $f = 0.7$).

The value of the $k_p/k_t^{1/2}$ parameter for NVP polymerizations in DMF is close to 0.23 ± 0.01 (L mol $s^{-1})^{1/2}$. This is in good agreement with the value calculated value from the study of Von Ekenstein et al.[33] who measured the apparent kinetic constant (i.e., $2k_p \cdot (f \cdot [I_0]/k_d \cdot k_t)^{1/2}$) for NVP polymerization in DMF with azabisisobutyronitrile (AIBN) as the initiator. Knowing the decomposition constant and the efficiency of AIBN at 70°C in DMF[34] ($f = 0.77$ and $k_d = 5.86\ 10^{-5}\ s^{-1}$), a $k_p/k_t^{1/2}$ value of 0.29 (L mol $s^{-1})^{1/2}$ was calculated. Anyway, these values are quite low compared to what has been observed in a solvent such as water[35] [$k_p/k_t^{1/2} = 2.3$ (L mol $s^{-1})^{1/2}$] (see Fig. 6). This drastic decrease of $k_p/k_t^{1/2}$ in DMF suggests that propagation and termination rate constants would be affected (differences in solvation compared to water). In addition, the chain transfer reaction could also interfere in the kinetics, producing an increase of k_t, especially if the reinitiation ability of transferred radicals is lower than the normal one. The chain transfer constant for a solvent (C_s) can be estimated from the well-known Lewis Mayo equation, as expressed in eq. (6):

$$\frac{1}{\overline{DP_n}} = \frac{1}{\overline{DP_{n_0}}} + C_s \cdot \frac{[S]}{[M]} \qquad (6)$$

where $\overline{DP_n}$ and $\overline{DP_{n_0}}$ are, respectively, the polymerization degrees with and without transfer; $[M]$ and

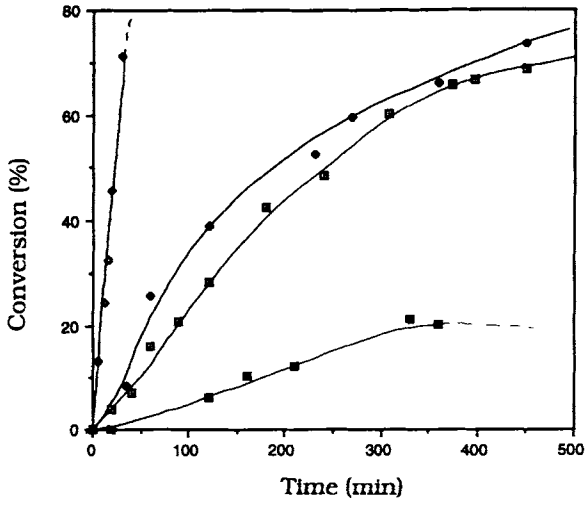

Figure 6 Typical conversion versus time curves for solution polymerization of NVP using ACPA, ACPS, and ACP-LC-B: (♦) GAF4; (□) GAF3; (■) GAF5; and (◇) NVP polymerization in water from Erout et al.[35]

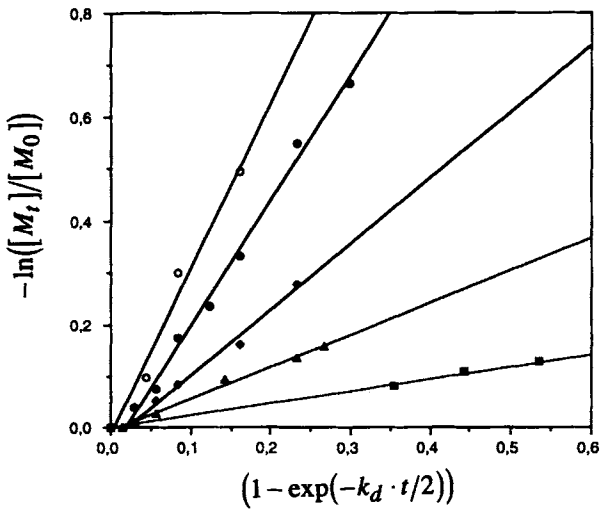

Figure 7 Data of $-\ln[M_t]/[M_0]$ as a function of $(1 - \exp(-k_d \cdot t/2))$ according to eq. (5). (▲) GAF1; (♦) GAF2; (●) GAF3; (○) GAF4; (■) GAF5.

Table VII Kinetic Values for Three Initiators Polymerization Experiments

References	Initiator Type	Monomer (mol L^{-1})	Conversion (%)	$\overline{M_n}$ (g mol^{-1})	$k_p/k_t^{1/2}$ (L mol $s^{-1})^{1/2}$
GAF1	ACPS	0.25	18	18,000	[a]
GAF2	ACPS	0.625	48	30,000	[a]
GAF3	ACPS	1.98	69	43,000	0.233
GAF4	ACPA	2.027	73.5	50,000	0.222
GAF5	ACP-LC-B	0.226	20.5	6,000	[a]

[a] Not calculated (initiator efficiency unknown).

[S] are, respectively, the monomer and solvent concentrations; and C_s is the transfer constant of the solvent.

From the three ACPS initiated polymerizations, the transfer constant has been determined by plotting $1/\overline{DP_n}$ versus $[S]/[M]$, as shown in Figure 8. It was found to be equal to 7.91 10^{-5} at 70°C, which is a high value. The molecular weight in the absence of transfer due to the solvent gives $\overline{M_{n_0}}$ = 53,600 g mol^{-1}. This transfer constant can explain the low polymer molecular weights, as shown in Table VII, but not the decrease in the overall conversions while decreasing the monomer concentration.

Then, knowing the $k_p/k_t^{1/2}$ ratio, all the initiator efficiencies (f) can be calculated from eq. (5); a variation of f is observed versus the monomer concentration,[36] especially for solutions with a low monomer content as reported in Table VIII. The plot of f versus $[M]/[I]$ (Fig. 9), where $[M]$ and $[I]$ are the monomer and initiator concentrations respectively, showed that, at low monomer concentration, initiator efficiency was rather weak. This phenomenon could be explained either by the preferential recombination of the two radicals' moieties issued from the initiator decomposition or because of a transfer between the radicals and the solvent. However, for a given concentration, the initiator efficiency reached a constant value, meaning that no disproportionation or transfer reaction occurs anymore (2 mol L^{-1} of NVP were necessary to reach 70% of conversion).

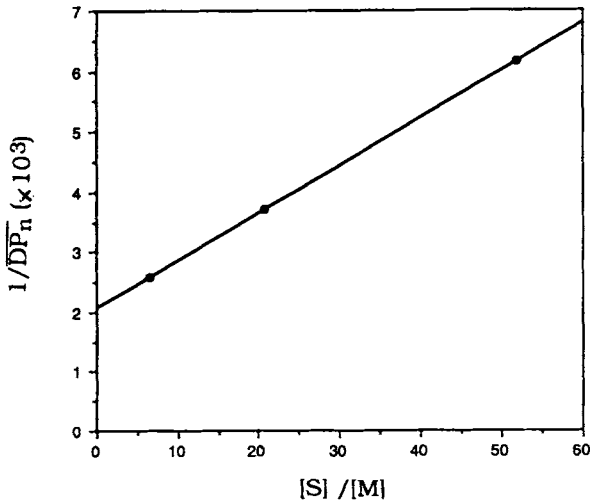

Figure 8 Data of $1/\overline{DP_n}$ versus $[S]/[M]$.

These results, in addition to the chain transfer reaction, can explain the low conversion obtained while decreasing the monomer concentration. In the case of ACP-LC-B initiated polymerizations, chain transfer reaction from the azoinitiator, bearing numerous labile protons, might be also responsible for the low molecular weight obtained. In addition, the higher decomposition rate of this initiator compared with the previous ones, and the lower efficiency would cause a significant decrease both in the polymerization rate and in the final conversion.

Titration of End Group Polymer Chains

ACPS. The detection and quantification of the NHS end groups in PVP was investigated using aqueous phase GPC.

This method was performed using the fact that hydrolysis of the end groups (by an excess of NH_4OH) induces a release of the NHS functions.

Table VIII Estimated Initiator Efficiencies

References	Initiator Type	Initiator Efficiency
GAF1	ACPS	0.29
GAF2	ACPS	0.58
GAF3	ACPS	0.70[a]
GAF4	ACPA	0.70[a]
GAF5	ACP-LC-B	0.17

[a] Literature value.[33]

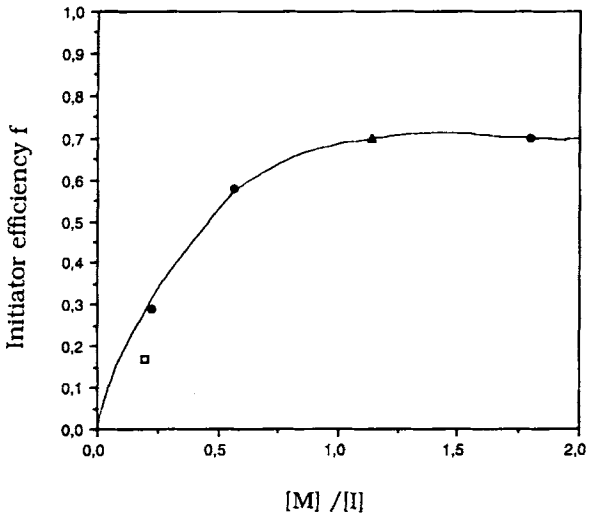

Figure 9 Plot of the initiator efficiency f depending on the monomer amount introduced in solution: (△) ACPA; (●) ACPS; (□) ACP-LC-B.

Furthermore, NHS exhibits a retention time different from that of the polymer. Then, by addition of a given amount of ACPS to ascertain the retention time of NHS, it was possible to assay the unknown quantity of NHS released by hydrolysis. The obtained values corresponding to three different concentrations of the GAF3 sample are reported in Table IX at two wavelengths (220 and 260 nm) and compared with the theoretical ones calculated from $\overline{M_n}$ = 43,000 g mol^{-1}, assuming the presence of one initiator fragment per polymer chain. This can be justified considering that most of the chains would terminate by chain transfer from the solvent.

Table IX Titration of NHS End-Groups by GPC in Aqueous Media (Sample GAF3)

Theoretical Concn (10^7 mol)[a]		2.20	0.95	0.38
Exp. concn (10^7 mol)	220 nm	17.00	7.25	0.13
	260 nm	2.30	1.20	0.21

[a] Calculated from the $\overline{M_n}$ of GAF3 sample, with one NHS end group per polymer chain.

More reliable results are obtained at 260 nm rather than at 220 nm due to the PVP peak absorption skew. It is worth noting that the observed values are close to the expected ones within experimental errors. Therefore, it may be concluded that the $\overline{M_n}$ of PVP deduced from aqueous phase GPC is reliable, and most of the polymer chains would contain an average number of ACPS fragments of one per chain, which assumes that transfer reaction from the solvent molecules mainly occurs on growing chains (compared to that involving initiator radicals).

ACP-LC-B. The aim of these experiments was to examine the changes in sensitivity of the immunoassay by varying the concentration of the antibody and of the selected polymer sample GAF5. The ACPS initiated polymer GAF3 was used as a ref-

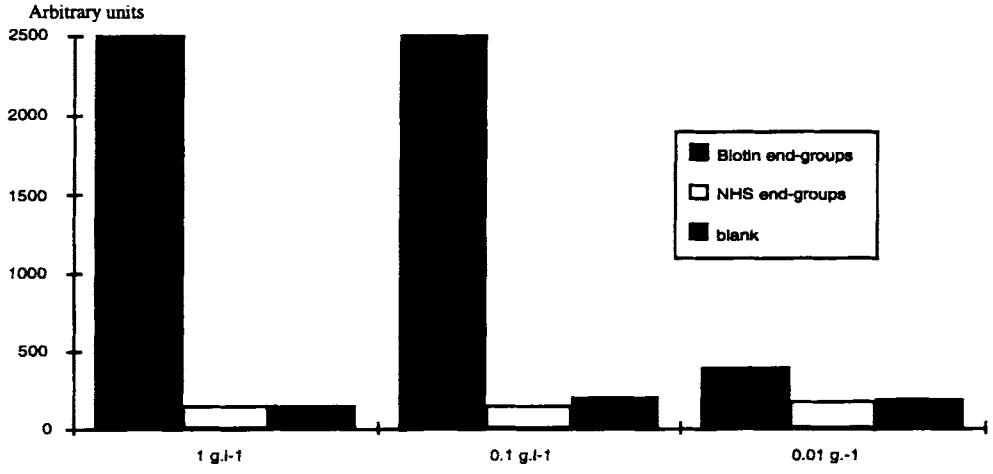

Figure 10 Colorometric values for the biotin/antibiotin antibody-HRP enzymatic reaction carried out for three polymer concentrations (respectively, 1, 0.1, and 0.01 g L^{-1}). Polymer samples engaged in these experiments were GAF5 (biotin end groups) and GAF3 (NHS end groups), respectively. Blank was realized without polymer.

erence to ensure that the antigen/antibody reaction was specific.

Two dilutions of antibody (1/100 and 1/250) in the PBS 3X/PBS horse serum solvent were used. Preliminary measurements indicated that the latter concentration was sufficient to perform the test. The results are compared in Figure 10, as a function of polymer amount necessary to perform the assay.

It should be noted that only the ACP-LC-B initiated polymer provides substantial results, that is, a subsequent optical density signal after the specific enzyme reaction, that is an indirect confirmation of the presence of the biotin end group in polymer GAF5. Furthermore, this test is very sensitive, because only 0.1 ng L^{-1} of polymer is needed to produce reliable and specific results. The capability of biotin to bind the associated antibody seems to not be altered by the polymer end group location, depending on how the polymer was adsorbed on the microplate.

CONCLUSION

The syntheses of new azoinitiators, succinimido (ACPS) and biotin (ACP-LC-B) derivatives, was performed using ACPA as the first reagent. These initiators are bifunctionalized as shown by spectroscopic methods such as UV or NMR spectroscopy. The NHS derivative exhibited the same decomposition behavior as ACPA as stated by a decomposition rate study performed by UV and DSC for ACPA and ACPS, respectively. The Arrhenius constants were measured as $\ln A = 35 \pm 1$ and 36 ± 2 and $E_a = 132 \pm 5$ and 140 ± 8 kJ mol^{-1} for ACPA and ACPS, respectively. The decomposition rate of the biotin derivative was performed by DSC, and gave lower energy activation ($E_a = 97 \pm 8$ kJ mol^{-1} and $\ln A = 25 \pm 2$) due to the steric hindrance of the biotin group. The polymerization of NVP by these initiators showed that ACPA and ACPS exhibited the same kinetic behavior, confirming the former results. The $k_p/k_t^{1/2}$ for NVP in DMF was calculated to be 0.23 ± 0.01 (L mol^{-1} $s^{-1})^{1/2}$, due to the fact that the DMF is a very active chain transfer agent; this transfer is also responsible for the low molecular weight values. Low conversions can be explained by initiator efficiencies that drastically vary with the initial monomer concentration; this proved a competition between recombination, transfer from the solvent to the initiated radicals, and propagation at low solid content. The ACP-LC-B initiated polymerization has a low conversion rate and provides a low molecular weight, showing that the biotin end groups might also play a role in transfer reaction. The presence of end groups on the polymer chain was proved by aqueous GPC for the ACPS initiated polymerization and by an original immunoassay for the biotin derivative. Therefore, it has been deduced that most of the polymer chains are monofunctionalized.

Work is in progress to prepare NVP based functional copolymers using these initiators. Such copolymers with different reactive functions should be suitable for covalently binding nucleic probes along the chain and anchoring the polymer chain onto a given support through its terminal group. Examples of such applications will be published later.[37]

The authors would like to thank the Service Central d'Analyse du CNRS (Solaize, France) for elemental analyses and mass spectroscopy measurements.

REFERENCES

1. S. F. Reed, *J. Polym. Sci. Part A-1*, **9**, 2029 (1971).
2. S. F. Reed, *J. Polym. Sci.: Polym. Chem. Ed.*, **11**, 1435 (1973).
3. S. F. Reed, *J. Polym. Sci.: Polym. Chem. Ed.*, **19**, 1863 (1981).
4. Y. Yagci and M. K. Mishra, in *Macromolecular Design: Concept and Practice*, Polymer Frontiers International Inc., New York, 1994, Chap. 6, p. 250.
5. I. Cakmak, *Macromol. Rep.*, **A31** (Suppl 3, 4), 333 (1994).
6. V. P. Kartavykh, V. A. Drach, Ye. N. Barantsevich, and Ye. L. Abramenko, *Polym. Sci. USSR*, **19**, 1413 (1977).
7. G. Clouet, M. Knipper, and J. Brossas, *Polym. Bull.*, **11**, 171 (1984).
8. Y. Hepuzer, M. Bektas, S. Denizligil, A. Onen, and Y. Yagci, *Macromol. Rep.*, **A30** (Suppl. 1, 2), 111 (1993).
9. M. A. Villalobos, A. E. Hamielec, and P. E. Wood, 3rd Int. Symp. Radical Copolym. Dispersed Media, Preprints 1994.
10. H.-R. Dicke and W. Heitz, *Colloid Polym. Sci.*, **260**, 3 (1982).
11. K. Tauer and S. Kosmella, *Polym. Int.*, **30**, 253 (1993).
12. B. Hazer, B. Erdem, and R. W. Lenz, *J. Polym. Sci.: Part A: Polym. Chem.*, **32**, 1739 (1994).
13. R. G. Santos, P. R. Chaumont, J. E. Herz, and G. J. Neinert, *Eur. Polym. J.*, **28**, 1263 (1992).
14. S. Denizligil and Y. Yagci, *Polym. Bull.*, **22**, 547 (1989).
15. C. G. Overberger and D. A. Labianca, *J. Org. Chem.*, **35**, 1762 (1970).
16. D. C. Blackley and A. C. Haynes, *J. Chem. Soc. Faraday Trans. I*, **75**, 935 (1978).
17. S. B. Idage, B. B. Idage, and S. P. Vernekar, *J. Appl. Polym. Sci.*, **45**, 931 (1992).

18. A. Onen, S. Denizligil, and Y. Yagci, *Angew. Makromol. Chem.*, **217,** 79 (1994).
19. Y. Yagci, U. Tunca, and N. Biçak, *J. Polym. Sci.: Polym. Lett. Ed.*, **24,** 49 (1986).
20. A. V. Lubnin and J. P. Kennedy, *J. Macromol. Sci.: Part A: Pure Appl. Chem.*, **A31,** 665 (1994).
21. R. C. Nowinski and A. S. Hoffman, U.S. Pat. 4,511,478 (1985) and 4,711,840 (1987).
22. K. Sugiyama, K. Ohga, and K. Kikukawa, *Macromol. Chem. Phys.*, **195,** 1341 (1994).
23. R. Barbucci, A. Magnani, C. Roncolini, and S. Silvestri, *Biopolymers,* **31,** 827 (1991).
24. T. Miron and M. Wilchek, *Anal. Biochem.*, **126,** 433 (1982).
25. O. Nuyken, J. Gerum, and R. Steinhausen, *Makromol. Chem.*, **180,** 1497 (1979).
26. I. M. Grumbach and R. W. Veh, *J. Immunol. Methods,* **140,** 205 (1991).
27. I. V. Berlinova, A. Amzil, S. Tsvetkova, and I. M. Panayotov, *J. Polym. Sci.: Part A: Polym. Chem.*, **32,** 1523 (1994).
28. E. Pretsch, T. Clerc, J. Seibl, and W. Simon, in *Tables of Spectral Data for Structure Determination of Organic Compound,* 2nd ed., Springer-Verlag, New York, 1989, p. C10.
29. E. Breitmaier and W. Voelter, *Carbon 13 NMR Spectroscopy,* 3rd ed., WCH, Germany, 1989, p. 91.
30. J. Brandrup and E. H. Immergut, *Polymer Handbook,* 3rd ed., Wiley–Interscience, New York, 1989, p. II.3.
31. J. M. Bessière, B. Boutevin, and O. Loubet, *Polym. Bull.*, **30,** 545 (1993).
32. J. M. H. Kusters, Ph.D. Thesis, Eindhoven University of Technology, The Netherlands, 1994.
33. G. O. R. Alberda Von Ekenstein, D. W. Koetsier, and Y. Y. Tan, *Eur. Polym. J.*, **17,** 845 (1981).
34. T. Fukuda, *Progr. Polym. Sci.*, **17,** 875 (1992).
35. M. N. Erout, A. Elaïssari, C. Pichot, and M. F. Llauro, *Polymer,* to appear.
36. G. Odian, *Principles of Polymerization,* 3rd ed., Wiley Interscience, New York, 1991, p. 236.
37. M. N. Frezet–Erout, Ph.D. Thesis, University of Lyon, Lyon, France, 1994.

Received February 23, 1995
Accepted April 25, 1995